

A THEORETICAL STUDY OF POTENTIAL ENERGY CURVES AND TRANSITION DIPOLE MOMENT OF THE CO⁺ ION

A. K. Jha*, A.Syiemiong, S. Swer and A. Saxena

Department of Physics, North-Eastern Hill University, Shillong-793022, India

*For correspondence. (ashok_phys@yahoo.co.in)

Abstract: Ab initio calculations were performed for several doublet states of the CO⁺ cation using the multi reference single and double excitation configuration-interaction (MRDCI) method. The dipole transition matrix elements for ²Σ⁺ and ²Π states have been calculated and the molecular properties of the CO⁺ cation have been studied in detail. The calculated results show good agreement of with available experimental measurements as well as other theoretical results.

Keywords: MRDCI; Potential energy surface; Spectroscopic constants; Transition dipole moment

PACS: 31.15.xr, 34.20.Gj.

1. Introduction:

The CO⁺ cation is one of the most important molecules in the study of astrophysics, atmospheric physics, plasma physics, environmental science and combustion processes [1]. It holds a very special place in the history of molecular ion spectroscopy. Its presence has been revealed in a number of different objects such as molecular clouds, stars, comet tails and planet atmospheres. On the one hand, the electronic spectra of the cation could enable us to understand the physical and chemical processes that take place in the solar and stellar atmospheres, comet tails and interstellar space; on the other hand, the cation has also been used as a monitoring probe for chemical dynamics in the investigation of environmental research and combustion processes.

Calculations of electronic transition moments between different electronic states are in general more complicated than calculations of properties of a single electronic state. This has to do with the fact that one either has to devise techniques for calculating the electronic transition moment between non-orthogonal wave functions or, if large CI expansions are employed, has to use one set of orthogonal molecular orbitals to describe both states. The complete active space self-consistent field [2] method has been particular useful for calculating non-orthogonal electronic transition moments. In this paper we present our theoretical adiabatic potential energy curves and transition dipole moment of the CO⁺ cation.

2. Results and discussion:

Ab initio calculation have been performed using the MRDCI method [3-6]. The atomic orbital set employed in this work consists of contracted Cartesian Gaussian functions. For carbon the aug-cc-pVQZ [7] basis set [6s,5p,4d,3f,2g] is contracted to [6s,5p,4d,3f] augmented with two diffuse s ($\alpha_s = 0.0230000$ and $0.0055000 a_0^{-2}$), two diffuse p ($\alpha_p = 0.021000$ and $0.0049000 a_0^{-2}$), and two diffuse d ($\alpha_d = 0.0150000$ and $0.0032000 a_0^{-2}$) orbit. For oxygen the augmented-cc-pVQZ [7] basis set [6s,5p,4d,3f,2g] is contracted to [6s,5p,4d,3f] augmented with two diffuse s ($\alpha_s = 0.0320000$ and $0.0022000 a_0^{-2}$), two diffuse p ($\alpha_p = 0.0310000$ and $0.0011000 a_0^{-2}$), and two diffuse d ($\alpha_d = 0.0150000$ and $0.0032000 a_0^{-2}$) are added into this contracted basis set.

A self-consistent field (SCF) calculation has been carried out for the ¹A₁ state at each internuclear distance considered in the present work. The resulting self-consistent field molecular orbitals (SCF-MOs) form the orthonormal one electron basis for the subsequent CI treatment. The adiabatic MRDCI energies have been calculated at 58 internuclear separation in the range $1.6 \leq R \leq 7 a_0$ (R is internuclear distance). The MRDCI method is employed with configurations selection and perturbative energy correction [3-6]. A set of reference configurations is chosen based on the preliminary scan of the wave function of the lowest root of a given symmetry at representative internuclear distances. The configuration interaction (CI) treatment itself is carried

out by employing the table CI method for efficient treatment of various open shell cases which arise because of single and double substitutions relative to the reference configurations.

A. Potential energy curves:

Fig.1 shows the potential energy curves (PEC) of CO^+ calculated by the aug-cc-PVQZ basis set. The potential energy curves lying below $70\,000\text{ cm}^{-1}$ relative to the $\nu = 0$ level of the $X^2\Sigma^+$ state are shown. These states dissociate to $\text{C}^+ (^2\text{P}) + \text{O} (^3\text{P})$ or $\text{C}^+ (^2\text{P}) + \text{O} (^1\text{D})$. From the figures we find that all of the calculated potential energy curves properly converge to the correct dissociation limit.

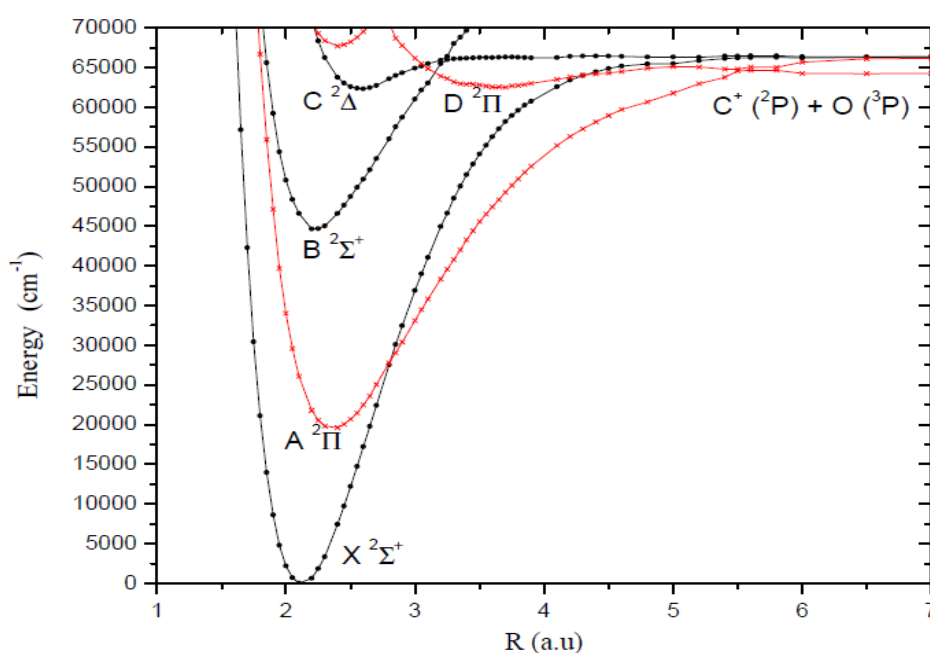


Figure 1: The potential energy curves of the $X^2\Sigma^+$, $A^2\Pi$, $B^2\Sigma^+$ states of CO^+ .

The most accurate value of the first ionization potential (IP) of CO, corresponding to $\text{CO}^+ (X^2\Sigma^+, v^+ = 0, N^+ = 0)$, was obtained by laser-induced fluorescence [8] as $14.013\,63 \pm 0.000\,04\text{ eV}$. This value corresponds to $T_e = 113\,028.33\text{ cm}^{-1}$. The best calculated value is that of Okada and Iwata of $112\,830\text{ cm}^{-1}$ [9]; our computed IP value is $112\,723.2\text{ cm}^{-1}$.

The $\text{CO}^+ (X^2\Sigma^+, A^2\Pi)$ MOs yielded a more compact description of the Rydberg states, thus facilitating the assignment of their character. Hence, the $1^1\Sigma^+$ states were computed employing the $\text{CO}^+ (X^2\Sigma^+)$ MOs and the $1^1\Pi$ state employing the $\text{CO}^+ (A^2\Pi)$ MOs. The $\text{CO}^+ (X^2\Sigma^+)$ state is described at the SCF level of approximation by $(1a_1)^2(2a_1)^2(3a_1)^2(4a_1)^2(1b_1)^2(1b_2)^2(5a_1)^1$ in C_{2v} symmetry and by $(1\sigma)^2(2\sigma)^2(3\sigma)^2(4\sigma)^2(1\pi)^4(1b_2)^2(5\sigma)^1$ in $C_{\infty v}$ symmetry, and $\text{CO}^+ (A^2\Pi)$ by $(\dots)(4a_1)^2(5a_1)^2(1b_1)(1b_2)^2$ in C_{2v} symmetry and by $(\dots)(4\sigma)^2(5\sigma)^2(1\pi)^3$ in $C_{\infty v}$. However, this choice is not without difficulties and implies compromises. The valence states, for instance, are less well described. Also, it is questionable whether the Rydberg-valence interaction is properly accounted for. With a single configuration, the $X^2\Sigma^+$, $A^2\Pi$, and the $B^2\Sigma^+$ state in the vicinity of their equilibria are best described by

$$\begin{array}{l} X^2\Sigma^+ \quad 1\sigma^2 2\sigma^2 3\sigma^2 4\sigma^2 1\pi^4 5\sigma^1, \\ A^2\Pi \quad 1\sigma^2 2\sigma^2 3\sigma^2 4\sigma^2 1\pi^3 5\sigma^2 \quad \text{and} \\ B^2\Sigma^+ \quad 1\sigma^2 2\sigma^2 3\sigma^2 4\sigma^1 1\pi^4 5\sigma^2 \end{array}$$

The first three σ orbitals which are predominantly oxygen 1s, carbon 1s and oxygen 2s were kept doubly occupied in the orbital optimization step. The minimal active space that allows for proper dissociation into $\text{C}^+ (s^2 p^1)$ and $\text{O} (s^2 p^4)$ consists of the $4\sigma, 5\sigma, 6\sigma$ and the 1π and 2π orbitals. Excitations from the oxygen 2s into the 3d orbital contribute significantly to the wave function of the atomic ^1D oxygen state to which the $B^2\Sigma^+$ state

dissociates. At $R_{CO} = 2.1 a_0$, near the equilibria of both $X^2\Sigma^+$ and $B^2\Sigma^+$, these excitations seem to be less important, however.

At large internuclear separations both the $X^2\Sigma^+$ and the $A^2\Pi$ molecular states correlate with the lowest dissociation channel, $C^+ (^2P_u) + O(^3P_g)$. Starting from the separated atoms, only the $A^2\Pi$ state can form a σ and a π bond while the $X^2\Sigma^+$ state is restricted by symmetry to build only a π bond. At long R_{CO} distances the $A^2\Pi$ state is therefore energetically located below the $X^2\Sigma^+$ state. At shorter internuclear separations strong s- p_σ hybridization on the carbon atom occurs in the $X^2\Sigma^+$ state. One of the hybrids is thus enabled to bind to the oxygen p_σ electron and the Coulomb repulsion is minimized by polarizing away the remaining electron from oxygen. Both effects then favour the $^2\Sigma^+$ state over the $^2\Pi$ state. The $B^2\Sigma^+$ state dissociates into $C^+ (^2P_u)$ and $O(^1D_g)$.

B. Transition dipole moment:

The calculated electronic transition moments μ_{AX} , μ_{BX} , and μ_{BA} as functions of the internuclear distance are displayed in fig. 2. Since the lifetime of the B state is dominated by the B-X transition only this decay channel will be discussed. The B-X moment has a marked maximum in the Franck-Condon region and falls off rapidly on both sides. The functional form of the B-X dipole transition matrix element can be understood in terms of electronic structure changes in the X and B states. The X and B states are well described by a single configuration at their respective equilibria. The excited state configuration $\dots 4\sigma^1 1\pi^4 5\sigma^2$ (b), can be generated from the ground state configuration $\dots 4\sigma^2 1\pi^4 5\sigma^1$ (a), by promotion of one electron, giving rise to a large dipole transition matrix element.

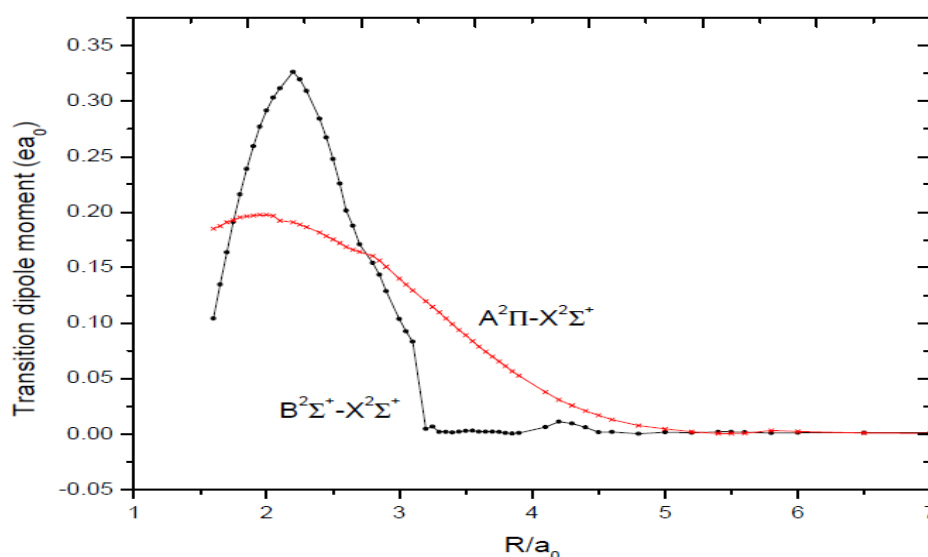


Figure 2: Calculated dipole transition moments for the $CO^+ A^2\Pi - X^2\Sigma^+$ and $B^2\Sigma^+ - X^2\Sigma^+$ transition

At somewhat longer bond distances, the ground state is still mainly characterized by configuration (a) while the B state mixes in considerable amounts of another low-lying configuration, $\dots 4\sigma^2 1\pi^3 5\sigma^1 2\pi^1$ (c). Both (b) and (c) are singly excited with respect to the ground state configuration (a), but enter the $B^2\Sigma^+$ state wave function with different signs such that their contributions to the transitions matrix element tend to cancel. This leads to the observed rapid decrease of the transition moment function with increasing internuclear distance.

At short internuclear separations, electronic wave function characteristics are more complicated. Comparison with the isoelectronic, homonuclear N_2^+ shows that in the united atom limit the electronic configuration of the $B^2\Sigma_u^+$ state correlates with the ground state of Si^+ while the $X^2\Sigma_g^+$ configuration leads to an excited state of Si^+ . Because of the presence of inversion symmetry, the $N_2^+ X^2\Sigma_g^+$ and $B^2\Sigma_u^+$ states retain their characters on crossing, therefore, the B-X transition CO moment remains essentially unchanged with decreasing internuclear separation [10]. In the heteronuclear CO^+ ion, and likewise in the CN molecule, this symmetry element is not present and the $B^2\Sigma^+$ states undergo an avoided crossing at short internuclear distance leading to a partial

cancellation of the terms contributing to the B-X transition moment. At the united atom limit, the transition moment should be different from zero, however. From the foregoing discussion it is clear that the height and location of the maximum of the B-X transition moment function are determined by a complicated balance of electronic configurations in the B and X states.

The A-X transition moment is only slightly R dependent, and turns gradually to zero as the internuclear separations grows. The same qualitative behaviour has previously been found by Rosmus and Werner [11] on the MC SCF level. Quantitatively, however their transition moment function has a steeper slope than ours.

3. Conclusion:

Using an appropriate set of molecular orbitals with an extensive basis set, we have demonstrated that multireference single and double configuration interaction (MRDCI) calculations provide accurate potential energy and dipole moment function curves for several low-lying electronic states. The calculated potential energy curves and transition dipole moment can be used for the experimentally unavailable data in simulating the microscopic and macroscopic properties of molecular gases. The electronic dipole transition moment functions of the $A^2\Pi - X^2\Sigma^+$, $B^2\Sigma^+ - X^2\Sigma^+$ transitions of CO^+ were calculated with highly correlated contracted CI wave functions.

References:

- [1] D. Shi, W. Li, J. Sun, Z. Zhu, Y. Liu, Computational and Theoretical Chemistry 978, 126-137, 2011.
- [2] B.O., Roos, P.R. Taylor and P.E.M. Siegbahn, Chem. Phys. 48, 157, 1980.
- [3] R. J. Buenker, and S. D. Peyerimhoff, Theoret. Chim. Acta 35, 33, 1974.
- [4] R. J. Buenker, Int.J. Quantum Chem. 29,435, 1986.
- [5] R. J. Buenker, in Proceedings of the Workshop on Quantum Chemistry and Molecular Physics, ed. P. G. Burton (University of Wollongong Press, Wollongong, Australia), p. 151, 1980.
- [6] R. J. Buenker, in Current Aspects of Quantum Chemistry 1981, edited by R. Carbo, Studies in Physical and Theoretical Chemistry Vol. 21, (Elsevier, Amsterdam), p 1781, 1982.
- [7] R.A. Kendall, T. H. Dunning Jr., and R. J. Harrison, J. Chem. Phys. 96, 6796, 1992.
- [8] A. Mellinger, C. R. Vidal, and Ch. Jungen, J. Chem. Phys. 104, 8913, 1988.
- [9] Kazutoshi Okada and Suehiro Iwata, J. Chem. Phys. 112, 22, 2000.
- [10] S.R. Langhoff and C.W. Bauschlicher, J. Chem. Phys. 88, 329, 1988.
- [11] P. Rosmus and H.-J. Werner, Mol. Phys. 47, 661, 1982.